

Cryogenic Single Crystal Silicon cavity

Jacques Millo, Clément Lacroûte, Alexandre Didier,
Enrico Rubiola and Yann kersalé
FEMTO-ST Institute
Besançon, France
millo@femto-st.fr

Julien Paris
MyCryoFirm
Paris, France
julien.paris@mycryofirm.com

Abstract—In this paper we present a study on an ultra-low noise cavity-stabilized-laser developed at the laboratory. The project aims to realize an ultra-stable cavity with a flicker frequency noise floor expected to be at $\sim 4 \times 10^{-17}$. This level of frequency noise can be achieved by making the cavity from a high mechanical quality factor material: single crystal silicon. The cavity needs to be cooled down to 17K with a cryocooled cryostat in order to cancel the coefficient of thermal expansion. Finite elements modeling helps to design a vibration insensitive cavity to be compatible with the objectives.

Keywords—cavity-stabilized-laser; single crystal silicon; vibration insensitive cavity; cryocooler cryostat

I. INTRODUCTION

Oscillators presenting the best short-term frequency stability are cavity-stabilized-lasers. The performances of such systems are limited by the thermal frequency noise of the ultra-stable cavity used as a frequency reference. Resulting fractional frequency stabilities in the low 10^{-16} decade and even below have been demonstrated [1]–[3]. The short term stabilities obtained with these ultra-stable lasers is currently the limit for the frequency stability of optical lattice frequency standards [1], [4], [5]. Consequently many research groups are working to reduce the effect of thermal noise in the reference cavities.

This limit stems from the Brownian thermomechanical noise in the components of the cavity (spacer, mirrors substrates and highly reflective coatings) and leads directly to fluctuations of the optical length that degrade the fractional frequency stability [6]–[8]. The reduction of the power spectral density of the displacement noise on each mirror can be achieved by decreasing the temperature of the cavity. The gain in term of fractional frequency stability is proportional of the square root of the temperature set point. For example, working at 17K instead of 300K leads to a gain of ~ 4 .

Another improvement is obtained by increasing the length of the cavity. For the same level of thermal noise, its relative contribution to the noise of the cavity decrease. For example, doubling the length provides a gain of a factor two on the fractional frequency stability. For this approach it is important to consider the sensitivity to vibrations of the cavity particularly if it is set in a cooling machine which is potentially a large source of vibrations. Nevertheless, increasing the length

of the cavity while maintaining low vibration sensitivity is a big challenge. Many groups have demonstrated cavities with low vibration sensitivity coefficients [9]–[14]. In a majority of cases the length of the cavity is at most two times the diameter for a diameter around 100 mm (or an equivalent cross section), *i.e.* an aspect ratio around 2. Unfortunately for vibration insensitive cavities, the size of the single bloc material available limits its diameter (or its cross section) and thus its length. A compromise has to be found between the length and the thermal noise level.

The thermal noise also depends on the mechanical quality factor of the material used to make the mirrors and the spacer of the cavity. In the last two years the largest gain has been obtained using single crystal silicon, leading to a gain of ~ 7 by comparison to an ULE cavity with fused silica substrates. An important characteristic in the choice of the material is the coefficient of thermal expansion. To fully take advantage of the improved short term frequency stability allowed by the low thermal noise it is important to cancel at the first order the temperature dependence of the cavity by setting the temperature at a zero-CTE. For the single crystal silicon it vanishes at $\sim 124\text{K}$ and $\sim 17\text{K}$. Let's also notice that transparency of this material is essential to making mirror substrates. It is the case for silicon for wavelengths around $1.5 \mu\text{m}$.

Following the impressive work realized by T. Kessler *et al.* [2] and later by E. Wiens *et al.* [15] we selected single crystal silicon as the best candidate to make the reference cavity. With a commercial pulse tube cryocooler the zero-CTE at 17K can be targeted. In this way a level of $\sim 4 \times 10^{-17}$ not yet demonstrated can be obtained with a cavity showing an aspect ratio about 1.5 and thus with a cavity more robust to vibrations and less costly.

II. CAVITY DESIGN

A. Context

The cryocooler cryostat used to cool down the ultra-stable cavity produces a high level of vibrations compared to ambient temperature cavities where a vibration isolation platform is used. The ultra-pure helium gas is compressed and expanded with a cycle of about 1 Hz. For commercially available cryocoolers the induced vibration produce displacements of 0.5

to 1 μm . This set an upper limit of the vibration sensitivity coefficients of $10^{-12} / (\text{m}\cdot\text{s}^{-2})$ to be compatible with the expected thermal noise. To release the constrains on that coefficient we develop a cryostat with a maximal displacement of 50 nm for 1 Hz frequency modulation, requiring less stringent coefficients of $2 \times 10^{-11} / (\text{m}\cdot\text{s}^{-2})$.

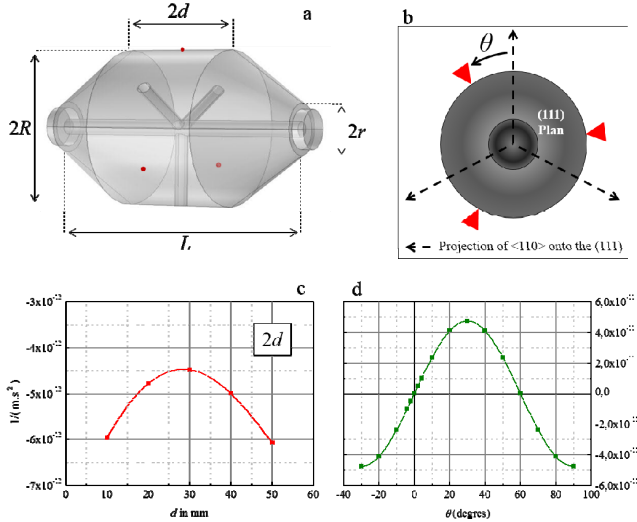


Fig. 1. a) Schematic of the single crystal silicon cavity ($d = 30$ mm, $r = 15$ mm, $R = 50$ mm, $L = 140$ mm). b) Representation of θ (side view of view a): angular mismatch between the contact points and projections of the $\langle 110 \rangle$ directions onto this (111) plan. c) Vibration sensitivity coefficient for transverse accelerations for 1 mm of the optical axis function of the parameter d . d) Vibration sensitivity coefficient for axial acceleration in the center of mirrors function of the parameter θ .

A practical and important aspect of the design is the absence of soft materials at cryogenics temperatures. For cavities working around room temperature soft materials like Viton® partially compensate the resulting forces between the cavity and the support and contribute to optimized symmetries. Consequently, it is not interesting to test the approach used in [9], [12], [16] for horizontal cavities at cryogenic temperatures. The vertically oriented cavities described in [2], [17], [14] are appropriate in this context. However, we decided to give the priority to a horizontally oriented cavity in order to simplify the realization of the low vibrations cryocooler cryostat.

B. Space Geometry

The spacer of the cavity is made from a single rod of low impurity single crystal silicon oriented along the [111] axis. As mentioned in [2] the plan (111) which is the plan of the cross section of the cylinder is anisotropic. One can identify three directions corresponding to the projections of the $\langle 110 \rangle$ directions onto this (111) plan with an angular periodicity of 120° . To maximize the number of symmetries the number of contacts points should be $3N$ (with N an integer) and have to be aligned to the specific directions mentioned just above.

The following optimization is performed using finite elements modeling with the software Comsol and with a similar approach as [9], [12], [16], [18].

To maximize the number of symmetries it has been decided to place the three contact points ($N = 1$) in only one vertical symmetry plan parallel to the (111) plan (see Fig. 1). The resulting forces from the support onto the cavity are automatically balanced if the three contacts are perfectly aligned to the specific directions. In that case, length changes measured between the centers of the mirrors for each direction of acceleration is null. Fig. 1 show the influence of an angular mismatch θ between the contact points and the crystalline specific directions. We notice the periodicity of 120° leading to two values of θ cancelling the coefficient: $\theta = 0^\circ$ correspond to an alignment of the contacts with the specific directions; $\theta = 60^\circ$ is the angular position which also conserve the symmetry by placing the contact on the bisecting line of the specific angular direction. The stiffness of this two directions is different by about 10%. The sensitivity to the angular alignment is $3 \times 10^{-12} (\text{m}\cdot\text{s}^{-2})^{-1}/\text{deg}$. The longitudinal centering sensitivity is $6 \times 10^{-12} (\text{m}\cdot\text{s}^{-2})^{-1} / \text{mm}$. This two sensitivities to the machining to the mounting is the most challenging aspect of this design.

For a given material, the mirror tilt induced vibration sensitivity strongly depends on the aspect ratio of the cavity for transverse accelerations. It can be reduced with a tapered shape of the cylinder [14]. The sensitivity due to the tilt of the mirror is optimized while varying the dimension $2d$ corresponding to the spacer length of constant diameter and varying r the radius of the tips of the spacer. First we observe that for a given value of d the lower sensitivity coefficient is obtained for $r = 15$ mm. Then, as shown on Fig. 1 30 mm is the best value for d and the corresponding coefficient of vibration sensitivity is $4.5 (\text{m}\cdot\text{s}^{-2})^{-1}$ for 1 mm off axis. This coefficient is improved by a factor two with respect to the simple cylinder and is the dominant term for the two transverse sensitivities.

III. CRYOCOOLER CRYOSTAT

To cool down the cavity we use a custom made cryocooler cryostat based on a commercial pulse tube Cryomech PT410 able to provide 1 W of cooling power for a temperature of $\sim 4\text{K}$. The cryostat is separated in two vessels connected together (see Fig. 2). The pulse tube is set under vacuum in the cooling vessel. A thermal shield is connected to the first cooling stage at 45K. Thus the cold head at the end of the pulsed tube is inside a first thermal shield. This second stage at 4K is connected to a very low thermal resistance heat transfer guide made in OFHC copper used for conductive heat exchange between the two parts of the cryostat. The cold head at 4K is connected to the heat transfer guide with flexible copper braids. The other side of this guide is located in the experimental part linked the cold plate with another set of copper braids. The cold plate is used to support the experiment protected by another thermal shield itself surrounded by another thermal shield thermalized to the first stage at 45K.

The space available for the experiment inside the shield is 250 mm diameter and 300 mm height. Vessel and shields are drilled and 3 pairs of AR coated windows are added for optical access. On the two shields they are made from fused silica for it has a lower thermal expansion coefficient than BK7, which is used for vacuum chamber windows. Getters at low temperature

allow a residual pressure below 10^{-8} mbar by cryopumping. A 25 L/s ion pump will be connected to the experimental vessel in order maintain the ultra-high vacuum level in case of breakdown of the cryocooler. This would avoid a degradation of the vacuum leading to fast temperature changes that could damage the cavity.

Using this concept which separates the cooling and the experiment a residual displacement lower than 50 nm has been measured (private communication). In a first test the temperature of the cold plate has been measured at ~ 4 K. To operate the cavity at ~ 17 K (the temperature of zero CTE) we have to warm up the supports and the shields of the cavity. Four heating elements (100 Ohms, 10 W resistors) are attached around a cylindrical support with 100 mm diameter and 34 mm height made with gold-coated OFHC copper. The dimensions and the materials are chosen to reduce temperature gradients. For heating efficiency this ensemble is screwed to the cold plate using six ring spacers in stainless steel showing an equivalent thermal resistance of 10K/W. Thus with 1 W to 1.5 W of heating power the temperature of cavity and its shielding should be between 15K to 20K.

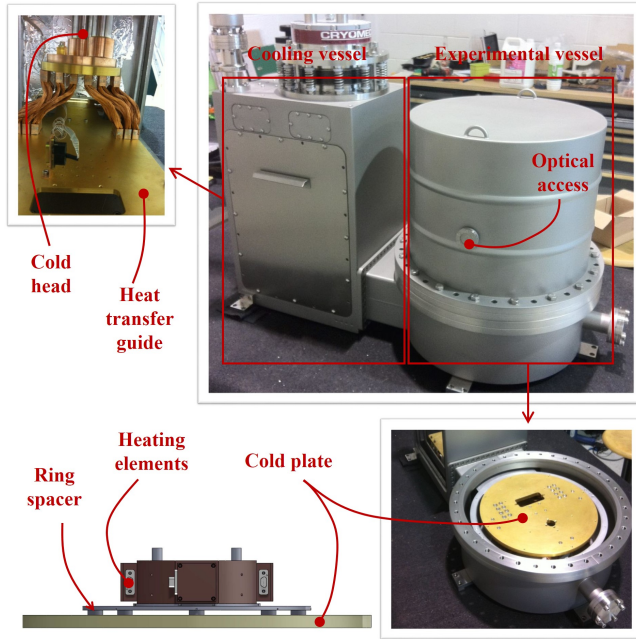


Fig. 2. Views of the cryocooler cryostat. Schematic of the setup design to temperature stabilize the cavity.

IV. DOPPLER EFFECT COMPENSATION

To measure the frequency detuning $\delta = \nu_l - \nu_c$ between the laser source ν_l and a resonance of the reference cavity ν_c one generally implements the Pound-Drever-Hall detection scheme (PDH). A feedback is applied to a laser frequency modulation to cancel the detuning. A fraction of the light is extracted using an output coupler. Many effects can produce changes of the optical length between the output coupler and the entrance mirror of the cavity. These are actually equivalent to an excess

phase noise of the laser beam which is detected and compensated by the loop filter correcting the frequency of the laser. Before the output coupler, this excess phase noise does not exist leading to a degradation of the cavity-stabilized-laser phase noise.

To achieve our ambitious targets we can point out two sources of Doppler frequency shifts able to degrade the frequency stability of the cavity-stabilized-laser. The first one is due to the residual displacement of the cavity 50 nm with a frequency of 1 Hz. The Doppler effect induces a fractional frequency shift on the laser wave probing the cavity by 10^{-15} in the hypothesis of a sine displacement. The second one is due to phase shifts induced by air flows, vibrations and temperature fluctuations between the output coupler and the input mirror of the cavity.

We propose an experimental setup to get rid of this problem. The idea is to build a Mach Zehnder interferometer (ZI) to measure and phase lock the phase fluctuations between the output coupler C in Fig. 3 and the cavity. One of the arms is the beam path from the splitter S of the ZI to the re-combiner R after reflection on the input mirror of the cavity. The second arm is the phase reference between S and R (Mach Zehnder Interferometer Reference Arm, ZIRA).

However the reference arm has to be very short to not integrate so much thermally-induced-length fluctuations and other phase noise fluctuations. In practice it will be more convenient to have this arm as long as needed for the optical set-up. The alternative consists of adding a Michelson interferometer (MI) with one short reference arm (Michelson Interferometer Reference Arm, MIRA) and a longer one. The phase of the longer one can be stabilized on the phase of the MIRA. Adding a splitter/combiner (S/C in Fig. 3) and semi-reflective wedge (W) in the ZIRA the long arm of the MI can build. Thus the phase noise in these two arms is the same and can be phase locked on the MIRA phase noise.

In practice it is more convenient to realize a heterodyne detection on the photodiode PD1 by placing an acousto-optic modulator (AOM) driven by a voltage controlled oscillator (VCO) at a frequency of $\sim f_0$ in the ZIRA. The phase noise is demodulated by a reference at a frequency of $2f_0$ and corrections are applied by modulating the VCO.

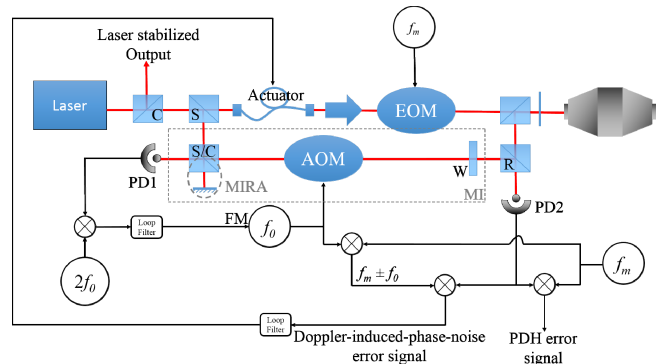


Fig. 3. Figure 1 Schematic of the Doppler effect compensation (PD: photodiode, C: output coupler, S: splitter, S/C: splitter/combiner, W: semi-

reflective wedge, R: re-combiner, MI: Michelson interferometer, MIRA: Michelson interferometer reference arm).

On the photodiode PD2 used to detect the frequency detuning in the PDH scheme the phase modulated field at angular frequency f_m and reflected by the cavity interferes with the field coming from the other part of the ZI.

Following the method detailed in [19] we calculate the power on the photodiode. We found the usual terms of PDH method. Two simplifications are made: first, for a phase modulation frequency larger than the cavity linewidth $\delta\nu$ the reflection coefficient is equal to -1 for frequencies of $\nu_l \pm f_m$; when the frequency detuning is smaller than the cavity linewidth, the reflection coefficient is approximated to $i\delta/(\pi\delta\nu)$.

With these simplifications three other terms appear. The first term at frequency f_0 is not useful because it vanishes when the laser is locked to the cavity ($\delta=0$). The two other terms contain information about the phase fluctuations: $2aJ_1(\beta)E_0^2 \cos(\pm 2\pi(f_m + f_0)t - \phi)$ with E_0 the magnitude of the electric field, ϕ the phase perturbation accumulated along the beam path and $J_n(\beta)$ the Bessel function of order n where β is the modulation index. The coefficient a is the fraction of the electric field that is coupled in the MI.

One is selected with band pass filtering and demodulated with a signal at frequencies ($f_m \pm f_0$). Phase corrections are applied on a phase or frequency transducer through a loop-filter (AOM, fiber stretcher, EOM or mirror mounted on a PZT) placed between the output coupler and the cavity.

V. CONCLUSION

In conclusion we presented the result of a study that aims to design a cavity-stabilized-laser with fractional frequency stability limited by the thermal noise at the level of $\sim 4 \times 10^{-17}$. A horizontal vibration insensitive cavity made from single crystal silicon with coefficient in the low $10^{-12} (\text{m.s}^{-2})^{-1}$ has been designed. We also presented the low vibration cryocooler cryostat that will be used to cool down the cavity to the zero of the coefficient of thermal expansion at $\sim 17\text{K}$. An optical setup is proposed in order to detect and compensate the frequency shifts induced by the Doppler effect taking its origin in the residual motion of the cavity and in the additional phase fluctuations induced on the beam coupled on the cavity.

ACKNOWLEDGMENT

We acknowledge the Agence National pour la Recherche together with the Conseil Régional of the region Franche-Comté founding this experiment, through the Oscillator IMP project. Thank to V. Giordano and S. Grop for the interesting and useful discussions about the cryostat. We also want to thank J. J. Boy for free access to the Goniometer.

REFERENCES

- [1] T. L. Nicholson, M. J. Martin, J. R. Williams, B. J. Bloom, M. Bishof, M. D. Swallows, S. L. Campbell, et J. Ye, « Comparison of Two Independent Sr Optical Clocks with 1×10^{-17} Stability at $10^{\pm 3} \text{ s}$ », *Phys. Rev. Lett.*, vol. 109, n° 23, p. 230801, déc. 2012.
- [2] T. Kessler, C. Hagemann, C. Grebing, T. Legero, U. Sterr, F. Riehle, M. J. Martin, L. Chen, et J. Ye, « A sub-40-mHz-linewidth laser based on a silicon single-crystal optical cavity », *Nat. Photonics*, vol. 6, n° 10, p. 687-692, 2012.
- [3] J. J. McFerran, D. V. Magalhães, C. Mandache, J. Millo, W. Zhang, Y. Le Coq, G. Santarelli, et S. Bize, « Laser locking to the 199Hg 1S0-3P0 clock transition with $5.4 \times 10^{-15} \text{ s}$ fractional frequency instability », *Opt. Lett.*, vol. 37, n° 17, p. 3477-3479, sept. 2012.
- [4] R. Le Targat, L. Lorini, Y. Le Coq, M. Zawada, J. Guéna, M. Abgrall, M. Gurov, P. Rosenbusch, D. G. Rovera, B. Nagórny, R. Gartman, P. G. Westergaard, M. E. Tobar, M. Lours, G. Santarelli, A. Clairon, S. Bize, P. Laurent, P. Lemonde, et J. Lodewyck, « Experimental realization of an optical second with strontium lattice clocks », *Nat. Commun.*, vol. 4, juill. 2013.
- [5] B. J. Bloom, T. L. Nicholson, J. R. Williams, S. L. Campbell, M. Bishof, X. Zhang, W. Zhang, S. L. Bromley, et J. Ye, « An optical lattice clock with accuracy and stability at the 10-18 level », *Nature*, vol. advance online publication, janv. 2014.
- [6] K. Numata, A. Kemery, et J. Camp, « Thermal-Noise Limit in the Frequency Stabilization of Lasers with Rigid Cavities », *Phys. Rev. Lett.*, vol. 93, n° 25, p. 250602, déc. 2004.
- [7] M. Notcutt, L.-S. Ma, A. D. Ludlow, S. M. Foreman, J. Ye, et J. L. Hall, « Contribution of thermal noise to frequency stability of rigid optical cavity via Hertz-linewidth lasers », *Phys. Rev. A*, vol. 73, n° 3, p. 031804, mars 2006.
- [8] T. Kessler, T. Legero, et U. Sterr, « Thermal noise in optical cavities revisited », *J. Opt. Soc. Am. B*, vol. 29, n° 1, p. 178-184, janv. 2012.
- [9] J. Millo, D. V. Magalhães, C. Mandache, Y. Le Coq, E. M. L. English, P. G. Westergaard, J. Lodewyck, S. Bize, P. Lemonde, et G. Santarelli, « Ultrastable lasers based on vibration insensitive cavities », *Phys. Rev. A*, vol. 79, n° 5, p. 053829, mai 2009.
- [10] S. Webster et P. Gill, « Force-insensitive optical cavity », *Opt. Lett.*, vol. 36, n° 18, p. 3572-3574, sept. 2011.
- [11] D. R. Leibrandt, M. J. Thorpe, M. Notcutt, R. E. Drullinger, T. Rosenband, et J. C. Bergquist, « Spherical reference cavities for frequency stabilization of lasers in non-laboratory environments », *Opt. Express*, vol. 19, n° 4, p. 3471-3482, févr. 2011.
- [12] T. Nazarova, F. Riehle, et U. Sterr, « Vibration-insensitive reference cavity for an ultra-narrow-linewidth laser », *Appl. Phys. B*, vol. 83, n° 4, p. 531-536, juin 2006.
- [13] J. Keller, S. Ignatovich, S. A. Webster, et T. E. Mehlstäubler, « Simple vibration-insensitive cavity for laser stabilization at the 10-16 level », *Appl. Phys. B*, p. 1-8, 2013.
- [14] A. D. Ludlow, X. Huang, M. Notcutt, T. Zanon-Willette, S. M. Foreman, M. M. Boyd, S. Blatt, et J. Ye, « Compact, thermal-noise-limited optical cavity for diode laser stabilization at 1×10^{15} », *Opt. Lett.*, vol. 32, n° 6, p. 641-643, mars 2007.
- [15] E. Wiens, Q.-F. Chen, I. Ernsting, H. Luckmann, U. Rosowski, A. Nevsky, et S. Schiller, « Silicon single-crystal cryogenic optical resonator », *Opt. Lett.*, vol. 39, n° 11, p. 3242-3245, juin 2014.
- [16] S. A. Webster, M. Oxborrow, et P. Gill, « Vibration insensitive optical cavity », *Phys. Rev. A*, vol. 75, n° 1, p. 011801, janv. 2007.
- [17] B. Argence, E. Prevost, T. Lévêque, R. Le Goff, S. Bize, P. Lemonde, et G. Santarelli, « Prototype of an ultra-stable optical cavity for space applications », *Opt. Express*, vol. 20, n° 23, p. 25409-25420, nov. 2012.
- [18] D. Guyomarc'h, G. Hagel, C. Zumsteg, et M. Knoop, « Some aspects of simulation and realization of an optical reference cavity », *Phys. Rev. A*, vol. 80, n° 6, p. 063802, déc. 2009.
- [19] E. D. Black, « An introduction to Pound-Drever-Hall laser frequency stabilization », *Am. J. Phys.*, vol. 69, n° 1, p. 79, 2001.